

1 **Performance of alkali activated slag concrete under aggressive environment**

2

3 **Corresponding Author: Parthiban Kathirvel**

4 School of Civil Engineering,

5 SASTRA University,

6 Thanjavur – 613 401,

7 Tamilnadu, India.

8 parthiban@civil.sastra.edu

9

10 **Saravana Raja Mohan Kaliyaperumal**

11 School of Civil Engineering,

12 SASTRA University,

13 Thanjavur – 613 401,

14 Tamilnadu, India.

15 srm@civil.sastra.edu

16

17 **Corresponding author:**

18 Tel.: +91-4362-264101; Mobile:; Fax: +91-4362-264120.

19 E-mail address: parthiban@civil.sastra.edu (Parthiban Kathirvel)

20

21 **Performance of alkali activated slag concrete under aggressive environment**

22 **Parthiban Kathirvel¹ and Saravana Raja Mohan Kaliyaperumal**

23 School of Civil Engineering, SASTRA University, Thanjavur – 613401, Tamilnadu, India.
24

25 **Abstract**

26 The environmental effects of production of Portland cement (PC) have provoked to examine the
27 growth of concrete with 100% replacement of cement with industrial byproducts containing high
28 amount of Si and Al, which are activated by alkali solutions termed as geopolymer concrete.
29 Concrete made with PC can be durable under mild exposure condition when properly designed
30 whereas undergo deterioration under severe exposure condition. Since very few works have been
31 performed on the ambient cured alkali activated slag concrete (AASC) under aggressive
32 environmental condition, this work was intended to study the effect of binder content and sodium
33 hydroxide concentration on AASC subjected to aggressive environment. In this regard, an
34 experimental investigation was carried out to study the influence of AASC under chloride, acid
35 and sulphate environment on its physical and mechanical properties. The results infer that the
36 AASC mixes perform well under aggressive environment condition.

37

38

39 **Keywords:** geopolymer concrete, alkali activated slag, aggressive environment, mechanical
40 properties, sulphate, chloride, ambient temperature.

41

¹Corresponding Author: Parthiban Kathirvel, Email: parthiban@civil.sastra.edu.

School of Civil Engineering, SASTRA University, Thanjavur – 613401, Tamilnadu, India.

Tele: +91 4362 264101, Mobile: +91 94435 32765, Fax: +91 4362 264120.

42 **1 Introduction**

43 The manufacture of PC needs huge amount of energy in the meantime transmits immense sum of
44 CO₂ to the atmosphere due to the calcination reaction during its manufacturing process. In the
45 manufacture of 1 T of PC, 0.53 T of CO₂ is released due to the calcination and may develop as
46 much as 1T if carbon gasoline is used as energy source. Conversely, the creation of commercial
47 through-products releases fewer amounts of green house gases (GHG) comparing to PC. Fly ash
48 produces 80-90 % and slag produces 80 % less GHG emission to the atmosphere compared with
49 PC. Therefore 100 % substitute of PC with fly ash or slag would significantly reduce the impact
50 on environment. In cement concrete, calcium silicate hydrate (C-S-H) and the portlandite
51 (Ca(OH)₂) are the chief hydration products which governs the strength and the binding
52 characteristics as well as highly susceptible to chemical degradation when exposed to severe
53 environmental conditions. This may also in some cases; that the configuration must be revamped
54 or even reinstated due to this effect. The dispersal of dissolved species inside interstitial fluid and
55 dissolution of diverse hydrate phases were the two processes suggested by Xie [1] to control the
56 degradation of cement-based materials under chemical exposure. Yang and Cho [2] expressed
57 that the accelerated chloride migration test showed a decent relationship linking the charge
58 passed and the steady state chloride flux. However, a new method based on Neumann's theory
59 was proposed by Chih-Hsing Wang [3] to determine the chloride diffusion coefficient without
60 the aid of electric current contrast to rapid chloride permeability test or rapid chloride migration
61 test. Cement concrete subjected to sulphate exposure is depicted by the chemical response of
62 sulphate particles as the forceful agent and the aluminate segment of hardened cement paste [4-
63 5]. The formation of ettringite due to high amount of C₃A is the main reason for the deterioration
64 of PC [6]. Among the properties that control the resistance to sulphate exposure, permeability

65 and chemical composition of cement paste are the most important. Due to the difference in the
66 chemical and phase composition, the concrete made with PC is more susceptible than made with
67 slag to acid attack. As a result of the formation of C-S-H gel and silica gel, the surface of the
68 cement concrete specimens becomes soft and could be delaminated resulting in concrete layers
69 to deterioration [7]. Alkali activated slag (AAS) mortar exposed to 5% sulphuric acid shows
70 severe degradation than citric acid, hydrochloric acid and nitric acid solutions over a period of 6
71 month [8]. The concrete made with AAS had superior resistance than concrete made with OPC
72 of similar grade when reacted with acetic acid solution of pH=4 [7].

73

74 Most of the previous studies have been done to study the behavior of geopolymer in the form of
75 mortar under aggressive environment when cured under elevated temperature. Since very few
76 researches were carried on geopolymer concrete under ambient temperature curing, this
77 experimental investigation was carried out to study the effect of binder content and NaOH
78 concentration on the physical and mechanical properties of AASC under aggressive
79 environment.

80

81 Hence, this paper at the inception provides an outline of the experimental investigation
82 integrating materials & their characteristics, their proportioning and experimental mechanism. It
83 was then pursued by an elaborated discussion on the obtained results, where the effect of
84 addition of binder content (350, 400 and 450kg/m³) and NaOH concentration (10, 12 and 14M)
85 on the physical and mechanical properties of the AASC under aggressive environment (acid,
86 sulphate and chloride) condition. The properties are offered in conjunction with added significant
87 elucidations.

88

89 **2 Materials and Methods**

90 **2.1 Constituent materials and mix proportion**

91 Ground granulated blast furnace slag (GGBFS) was used as geopolymer source material (GSM),
92 as GGBFS is the most common cementitious material for AAS binder [9] and its chemical
93 composition is given in Table 1.

94

95 From Table 1, the slag used was categorized as acidic, as the ratio between the total basic to
96 acidic components was found to be 0.98 which makes it best suited as a starting material for
97 AAS binder. The past research works suggested that the blend of sodium hydroxide (NaOH) and
98 sodium silicate (Na_2SiO_3) solution can be used as alkali activators resulting in higher strength
99 [10]. Sodium hydroxide was acquired in the form of flakes and sodium silicate in liquid form
100 with silica modulus of 2.5. The fine and the coarse aggregates were equipped in accordance with
101 ASTM C33/C33M (*Standard Specification for Concrete Aggregates, ASTM International, 2016*)
102 and their moisture condition was found to be in saturated surface dry (SSD) condition. Graded
103 river sand with a fineness modulus of 2.56 and specific gravity of 2.58 was used as fine
104 aggregates along with the coarse aggregate of 16mm maximum size of crushed granite type
105 available in saturated surface dry condition with a fineness modulus of 6.70 and specific gravity
106 of 2.61. To evaluate the performance of the mixes under aggressive environment condition, the
107 AASC mixes were prepared with variation in the volume of GGBFS as 350, 400 & 450 kg/m^3
108 and the NaOH concentration as 10, 12 and 14 molar, keeping the molar ratio of $\text{SiO}_2/\text{Al}_2\text{O}_3$ and
109 liquid to binder ratio constant and the mix proportions are shown in Table 2.

110

111 **2.2 Methodology**

112 The workability of the mixes was determined in the form of slump cone test following ASTM
113 C143/C143M (*Standard Test Method for Slump of Hydraulic-Cement Concrete, ASTM*
114 *International, 2015*). The compressive strength was determined using cylindrical specimens of
115 size 100mm dia. and 200mm height as per ASTM C39/C39M (*Standard Test Method for*
116 *Compressive Strength of Cylindrical Concrete Specimens, ASTM International, 2015*). The
117 moisture absorption and volume of voids were ascertained using 100mm size cubes as per
118 ASTM C642 (*Standard Test Method for Density, Absorption and Voids in Hardened Concrete,*
119 *ASTM International, 2013*). Exposure to acid attack was chosen to study its durability
120 characteristics as the acids are normally considered to be highly aggressive to concretes. The
121 sulphuric acid is taken into the account as this combines both acidic and sulphate environment
122 simultaneously. The percentage variation in mass and compressive strength of the mixes made
123 with 100 mm cubes exposed to 2% sulphuric acid over a period of 90 days were assessed as
124 considered by Li and Zhao [11]. The chloride ion diffusion was measured using salt ponding test
125 similar to the test prescribed in AASHTO T259 (*Standard Method of Test for Resistance of*
126 *Concrete to Chloride Ion Penetration (Salt Ponding Test), American Association of State*
127 *Highway and Transportation Officials, 2002*) and AASHTO T260 (*Standard Method of Test for*
128 *Sampling and Testing for Chloride Ion in Concrete and Concrete Raw Materials, American*
129 *Association of State Highway and Transportation Officials, 2009*) using cylindrical specimens
130 of 100mm dia. and 200mm height and the potentiometric titration was carried out as per NT
131 BUILD 208 (*Concrete, hardened: Chloride content by Titration, Nord Test Method, 3rd Edn.,*
132 *2011*) to determine the total chloride content (%) by weight of concrete using Eq. (1).

133

134
$$\text{Total Chloride Content (Cl}^-) = 3.545 \times \frac{V_1 N_1 - V_2 N_2}{m} \quad (1)$$

135

136 where, V_1 and N_1 are the volume and normality of AgNO_3 solution added, V_2 and N_2 are the
137 volume and normality of ammonium thiocyanate added.

138

139 The resistance to sulphate attack was evaluated using cylindrical specimens of size 100mm dia.
140 and 200mm height following ASTM C88 (*Standard Test Method for Soundness of Aggregates by*
141 *use of Sodium Sulfate or Magnesium Sulfate, ASTM International, 2013*). The specimens were
142 immersed in 5% sodium and magnesium sulphate solutions over a period of 90 days and the
143 reduction in mass and strength were evaluated. The core samples of 50mm height were taken for
144 visual examination. The solutions were changed periodically at an interval of 10 days in order to
145 maintain the concentration throughout the exposure period. The loss in the strength was
146 measured by sulphate deterioration factor (SDF) which is the percentage variation in strength of
147 the specimens after immersion in sulphate solution with that of immersed in water at age “t”.

148

149 **3. Results and discussion**

150 **3.1. Fresh concrete properties**

151 The workability of concrete is mainly influenced by the water requirements at the time of
152 mixing. For conventional concrete, it was decided mainly on the basis of the maximum size of
153 aggregate used. The test results of the workability of the AASC mixes are presented in Fig 1. As
154 can be seen, the workability of AASC mixes decreased when NaOH concentration increased. A
155 clarification for this pattern can be because of the measure of water and alkaline in the solution
156 prepared. More NaOH solids were allowed with the increase in the activator concentration and

157 less free water for a given volume, bringing about the reduction in the slump values. Similarly,
158 the slump values were observed to reduce with the increase in the GGBFS volume similar to
159 OPC concrete.

160

161 **3.2 Compressive strength**

162 The compressive strength results of the AASC mixes at the age of 7 and 28 days curing are
163 shown in Fig 2 and 3 respectively. The use of high calcined source material as binder was stated
164 to improve the microstructure of the geopolymer matrix resulting in high strength [12] and the
165 reaction between GGBFS and alkaline solution is an exothermal process in which the
166 geopolymerization process will be promoted by the generated heat [13]. GGBFS contains higher
167 CaO content and consequently, it is a good impending resource of soluble Ca in the mixture. The
168 amount of soluble calcium relies on the GGBFS quantity available in the mix and the
169 compressive strength has a direct consequence on it. An increase in the compressive strength
170 results was found to be averagely 12.9 % for 7 days and 11.8 % for 28 days curing with an
171 increase in the GGBFS content of 350 to 400 kg/m³ and drops averagely by 3.8 % for 7 days and
172 3.4 % for 28 days curing when increase to 450 kg/m³.

173

174 The activator concentration has been known as the most critical component influencing the
175 properties of alkali-activated binders. The impacts of activator concentration, in any case, have
176 not generally been that basic. While a few studies proposed that a base minimum concentration
177 of activators are required for the activation to be successful, there are distinctive studies
178 demonstrating adverse impacts of high concentration on the strength properties of alkali-
179 activated binders. The utilization of high concentration NaOH solution increases the dissolution

180 of the solid materials and the geopolymerization process resulting in higher compressive strength
181 and mostly because of the higher level of leaching of Si and Al. NaOH concentration on aqueous
182 phases increases the compressive strength averagely by 13.0% and 12.9% for 7 and 28 days
183 curing respectively for an increase in the NaOH concentration of 10M to 12M; and further
184 increment in the strength averagely by 11.5% and 12.1% for 7 and 28 days curing respectively
185 from 12M to 14M. Since one of the fundamental strides of geopolymerization procedure is the
186 breakdown of aluminosilicate bonds (Si-O-Si and Al-O-Si) in alkaline environment, higher
187 concentration prompted enhanced breakdowns. As more breakdown of aluminosilicate bonds,
188 there were further prospects for hydrates to be shaped, thus increasing the compressive strength.
189 The increase in the compressive strength with the increase in the NaOH concentration can be
190 related to improved solvency of aluminosilicate at higher concentration [14-15].

191

192 **3.3 Saturated water absorption and volume of voids**

193 The variation in the water absorption and the volume of voids of the AASC mixes are shown in
194 Fig 4 and 5 respectively. The amount of binder content in concrete has an especially strong
195 impact on the water retention properties of AASC mixes, despite the fact that the absorption
196 characteristics are, in all cases, lower than the equivalent OPC mixes even where porosities are
197 comparative. This is most likely a consequence of the presence of exceptionally refined,
198 convoluted and confined porosity in the AASC samples, which water does not promptly
199 infiltrate, furthermore the continuous arrangement of reaction products at advanced ages of
200 curing [16].

201

202 The superior property of the volume of voids is mainly because of the structure of the C-A-S-H
203 (CaO-Al₂O₃-SiO₂-H₂O) binding gel type which dominates the microstructure of the geopolymer
204 concrete is highly dense [17] comparing to N-A-S-H (Na₂O-Al₂O₃-SiO₂-H₂O) gel formed in fly
205 ash based GPC and C-S-H gel [18] formed in conventional cement concrete. The existence of
206 added bound water, persuaded by the availability of Calcium ion in the network, offers superior
207 pore-filling ability to C-A-S-H gel than N-A-S-H type gels in GPC [19].

208

209 **3.4 Resistance to sulphate attack**

210 **3.4.1 Sulphuric acid attack**

211 The percentage reductions in mass and compressive strength results are shown in Fig 6 and 7
212 respectively. The excellent acid resistance performance is mainly owing to the absence of
213 Ca(OH)₂. Unlike concrete made with PC which relies on C-S-H bonds for structural integrity,
214 geopolymers are novel binders that depend on aluminosilicate for structural integrity and hence
215 reported as acid resistant. High content of binder leads to reduction in deterioration of specimens
216 and found structurally intact with no appreciable change in colour. This excellent performance
217 may also be associated to the formation of alumino-silicate gel as the main binder in AASC
218 mixes which generally does not have free lime [7]. Greater resistance to sulphuric acid of GPC in
219 general has been stated by Thokchom et al., [20].

220

221 The AASC specimens were found to remain structurally intact without any significant variation
222 in mass and compressive strength. Even after 90 days, the AASC specimens were structurally
223 sound without any surface deterioration.

224

225 **3.4.2 Sodium and Magnesium sulphate attack**

226 The percentage variation in mass loss and strength loss of the AASC mixes after exposure to 5%
227 Na_2SO_4 solutions are shown in Fig 8 and 9 respectively and that of under MgSO_4 exposure are
228 shown in Fig 10 and 11 respectively. The maximum reduction in the mass of the AASC mixes
229 was found to be 2.54% and 4.57% under Na and Mg sulphate solutions respectively and that of
230 the compressive strength was observed to be 8.06% and 13.15% respectively. Some of the past
231 researches [21-23] showed that there is a gain in the mass of the specimens under Na sulphate
232 solution, whereas the present investigation shows a slight reduction in the mass under Na
233 sulphate environment. This may be due to the ambient curing condition followed in this work
234 unlike elevated curing techniques adopted in the past researches, where the liquid present in the
235 pores will be evaporated leaving the pores to be filled by the sulphate attacking agents resulting
236 in mass gain [23]. The gain in the mass is also associated with the expansion of the specimens,
237 when the pores are filled with sulphate attacking agents like gypsum and ettringite [24].

238

239 It has been noted that the percentage reduction in mass and compressive strength decreases with
240 the increase in the NaOH concentration. High concentration of NaOH might be the reason for the
241 arrangement of increasing amount of dense sodium-alumino-silicate gel in the network and rate
242 of geopolymerization thereby improved performance. The absence of Gypsum & Ettringite
243 results in no significant reduction in mass loss and strength degradation of the AASC mixes. The
244 specimens were found to maintain their integrity with no distress observed on the surface when
245 examined visually. The specimens were subjected to increased amount of distress in MgSO_4
246 solution comparing to Na_2SO_4 solution. After 90 days of exposure, there were some cracks on
247 the corners were observed and the degradation might be due to the presence of Gypsum and the

248 release of alkalis from geopolymers into the solution in AASC. No formation of ettringite was
249 observed as the slag is rich in aluminum that is not in the form available for the reaction.

250

251 Fig 12 shows the exposed specimens under Na and Mg sulphate environment after 90 days. As
252 the percentage variation in mass of the AASC specimens exposed to sodium and magnesium
253 sulphate solutions are negligible, this cannot be taken as a reliable sign of deterioration by
254 sulphate attack. Conversely, there is a considerable reduction in the compressive strength was
255 observed with the sulphate exposure which can be taken as a measurable indicator of
256 deterioration. It was observed that the specimens immersed in Na_2SO_4 solution shows exposition
257 of grains alone whereas the specimens in MgSO_4 solutions shows both exposition and dissolved
258 aluminosilicate matrix, which implies the rigorousness of Mg ions [25].

259

260 **3.5 Chloride penetration**

261 **3.5.1 Chloride content profile**

262 Various strategies are available to assess the chloride ion diffusion in OPC concretes, frequently
263 offers an electrical field to drive the chloride ion transportation in the samples. At the point when
264 these techniques are utilized to assess the geopolymer frameworks, the electrical potential is
265 required to accelerate the ion transportation through the pore system because of increased Na^+
266 concentration present in the pore arrangement [26]. Therefore, the chloride diffusion mechanism
267 can be affected altogether. In this way, these accelerated tests are viewed as temperamental,
268 when contrasting frameworks and generously diverse pore arrangements [27]. The long term
269 investigation of chloride ion penetration in AASC mixes was attempted as the accelerated
270 methods were proved to be futile, since a rise in temperature during test was exhibited in

271 geopolymer specimens is against the Ohm's law [28]. Salt ponding technique can be used to
272 assess the chloride ion penetration under non-accelerated conditions as per ASTM C1202
273 (*Standard test method for electrical indication of concrete's ability to resist chloride ion*
274 *penetration, ASTM International, 2008*). The chloride content profiles of the AASC mixes are
275 shown in Fig 13 to 15.

276

277 From the Figs, it has been observed that the reduced absorption capacity of the AASC mixes was
278 mainly due to the high tortuous nature of the aluminosilicate phase of AASC than the porous
279 microstructure of fly ash based geopolymer mixes [19]. The reason that related to the reduced
280 porosity and pore sizes and improved tortuosity has been discussed at the above. The chloride
281 ingress can also be further reduced with the extended age of curing [27] due to the reduced
282 permeability and sorptivity. The results reveal that the increase in the NaOH concentration
283 reduced the chloride ion diffusion. The increase in the NaOH concentration leads to the increase
284 in the compressive strength of geopolymer mixes due to dense matrix, thereby reduction in the
285 porosity resulting in less chloride ingress. Generally, alkali with high concentration dissolves
286 high proportion of source material due to higher degree of geopolymerization resulting in dense
287 microstructure in the system, thereby reducing the chloride ion ingress in AASC mixes with
288 higher NaOH concentration. In general, the mixes made with AAS has almost zero Ca(OH)_2 [29]
289 and pores of lesser size than OPC results in lower permeability, results in protection from the
290 ingress of deleterious ions.

291

292 **3.5.2 Chloride Diffusion Coefficient (D_c)**

293 The chloride profile from the tested specimens was used to compute the chloride diffusion
294 coefficient (CDC) and the results are detailed in Table 3. In the present study, the chloride
295 diffusion coefficient (D_c) has been computed using Fick's second law of diffusion which is given
296 by Eq. (2).

$$298 \frac{\partial c}{\partial t} = D_c \frac{\partial^2 c}{\partial x^2} \quad (2)$$

299 where, C is the concentration of chloride ions as a function of distance x , at any time t , and
300 D_c is the diffusion coefficient.

301
302 This is helpful in predicting the time required for protecting the concrete from corrosion
303 presuming a threshold rate in depassivating the steel reinforcement and thereby the initiation of
304 corrosion. The CDC values were found to reduce with the increase in the NaOH concentration
305 and slag content. The improved resistance to chloride penetration is mainly due to the refined
306 pore structure, which confines the diffusion of chloride ions into the samples [30]. The CDC
307 values were also observed to get reduced with the increase in the slag content. This is due to the
308 high refinement of pore microstructure with increased amount of slag content thereby reducing
309 the ingress of aggressive agents. Due to the very low CDC values for AASC mixes, it can be
310 accepted that the time required for depassivation of steel in AASC is higher than cement
311 concrete.

312

313 **4 Conclusions**

314 By analyzing the concrete mixes prepared at a range of sodium hydroxide concentration and
315 binder content, using alkali activated slag as binder, the mechanical properties and behavior

316 under aggressive environment have been determined. From the experimental results obtained, the
317 following conclusions can be made:

- 318 1. The compressive strength of the AASC mixes increases with the increase in the NaOH
319 concentration.
- 320 2. The AASC mixes shows superior mechanical and durability properties under aggressive
321 environment.
- 322 3. There is less evident of microcracking was observed in AASC mixes even at higher
323 binder content, which is mainly due to the lower amount of heat release in AASC mixes
324 comparing to OPC mixes.
- 325 4. The performance of the AASC mixes was also improved with the increase in the NaOH
326 concentration which is mainly due to the improved polymerization products at higher
327 concentration.
- 328 5. The excellent resistance of the AASC mixes under acid environment is mainly due to the
329 very low calcium oxide content and that of the sulphate environment is mainly due to the
330 absence of sulphate deteriorating factors.
- 331 6. The reduced pore size and improved tortuous nature of AAS confines the diffusion of
332 chloride ions into the samples.
- 333 7. In general, the mixes made with AAS has almost zero calcium hydroxide and pores of
334 lesser size than OPC results in lower permeability, results in protecting the concrete from
335 the ingress of deleterious ions.

336

337 **Acknowledgement**

338 The authors acknowledge the Vice Chancellor, SASTRA University, Thanjavur, India for
339 providing the facilities to carry out the work and the encouragement in completing this work.

340

341 **References**

342 [1] Xie, S.Y., Shao, J.F. and Burlion, N. “Experimental study of mechanical behaviour of cement
343 paste under compressive stress and chemical degradation”, *Cem. Concr. Res.*, **38**(12), pp. 1416-
344 1423 (2008).

345

346 [2] Yang, C.C. and Cho, S.W. “The relationship between chloride migration rate for concrete and
347 electrical current in steady state using the accelerated chloride migration test”, *Mater. Struct.*, **37**,
348 pp. 456-463 (2004).

349

350 [3] Wang, C.H., Tsai, C.L. and Lin, C.C. “Penetration lag of chloride diffusion through concrete
351 plate based on advancing model”, *J. Mar. Sci. Tech.*, **19**(2), pp. 141-147 (2011).

352

353 [4] Rasheeduzzafar, Dakhil, F.H., Al-Gahrani, A.S., Al-Saadoun, S.S. and Bader, M.A.
354 “Influence of cement composition on the corrosion of reinforcement and sulfate resistance of
355 concrete”, *ACI Mater. J.*, **87**(2), pp. 114-122 (1990).

356

357 [5] Rasheeduzzafar, Al-Amoudi, O.S.B., Abduljanwad, S.N. and Maslehuddin, M. “Magnesium-
358 sodium sulfate attack in plain and blended cements”, *J. Mater. Civil. Eng.*, **6**(2), pp. 201-222
359 (1994).

360

361 [6] Gollop, R.S. and Taylor, H.F.W. “Microstructural and microanalytical studies of sulfate
362 attack: I. Ordinary Portland cement paste”, *Cem. Concr. Res.*, **22**(6), pp. 1027-1038 (1992).

363

364 [7] Bakharev, T., Sanjayan, J.G. and Chen, Y.B. “Resistance of alkali-activated slag concrete to
365 acid attack”, *Cem. Concr. Res.*, **33**(10), pp. 1607-1611 (2003).

366

367 [8] Jiang, W., Silsbee, M.R., Breval, E. and Roy, D.M. “Alkali activated cementitious materials
368 in chemically aggressive environments”, in: K.L Scrivener, J.F. Young, *Mechanisms of*
369 *Chemical Degradation of Cement-Based Systems*”, E & FN Spon, London (1997).
370

371 [9] Wang, S.D. and Scrivener, K.L. “Hydration products of alkali activated slag cement”, *Cem.*
372 *Concr. Res.*, **25**(3), pp. 561-571 (1995).
373

374 [10] Yang, K.H., Song, J.K., Ashour, A.F. and Lee, E.T. “Properties of cementless mortars
375 activated by sodium silicate”, *Constr. Build. Mater.*, **22**(9) pp. 1981-1989 (2008).
376

377 [11] Li, G. and Zhao, X. “Properties of concrete incorporating fly ash and ground granulated
378 blast-furnace slag”, *Cem. Concr. Compos.*, **25**(3), pp. 293- 299 (2003).
379

380 [12] van Jaarsveld, J.G.S., van Deventer, J.S.J. and Lukey, G.C. “The effect of composition and
381 temperature on the properties of fly ash- and kaolinite-based geopolymers”, *Chem. Eng. J.*, **89**(1-
382 3), pp. 63-73 (2002).
383

384 [13] Ridtirud, C., Chindapasirt, P. and Pimraksa, K. “Factors affecting the shrinkage of flyash
385 geopolymers”, *Int. J. Miner. Metall. Mater.*, **18**(1), pp. 100-104 (2011).
386

387 [14] Bondar, D., Lynsdale, C.J., Milestone, N.B., Hassani, N. and Ramezani pour, A.A.
388 “Engineering properties of alkali-activated natural Pozzolan concrete”, *ACI Mater. J.*, **108**(1),
389 pp. 64-72 (2011).
390

391 [15] Khale, D. and Chaudhary, R. “Mechanism of Geopolymerization and Factors Influencing Its
392 Development: a Review”, *J. Mater. Sci.*, **42**(3), pp. 729-746 (2007).
393

394 [16] Bernal, S.A. and Provis, J.L., de Gutierrez, R.M., Rose, V. “Evolution of binder structure in
395 sodium silicate-activated slag-metakaolin blends”, *Cem. Concr. Compos.*, **33**(1), pp. 46-54
396 (2011).
397

- 398 [17] Ismail, I., Bernal, S.A., Provis, J.L., San Nicolas, R., Hamdan, S. and van Deventer, J.S.J.
399 “Modification of phase evolution in alkali-activated blast furnace slag by the incorporation of fly
400 ash”, *Cem. Concr. Compos.*, **45**, pp. 125-135 (2014).
401
- 402 [18] Lothenbach, B., Scrivener, K. and Hooton, R.D. “Supplementary cementitious materials”,
403 *Cem. Concr. Res.*, **41**(12), pp. 1244-1256 (2011).
404
- 405 [19] Provis, J.L., Myers, R.J., White, C.E., Rose, V. and van Deventer, J.S.J. “X-ray
406 microtomography shows pore structure and tortuosity in alkali-activated binders”, *Cem. Concr.*
407 *Res.*, **42**(6), pp. 855-864 (2012).
408
- 409 [20] Thokchom, S., Ghosh, P. and Ghosh, S. “Effect of Na₂O Content on Durability of
410 Geopolymer Mortars in Sulphuric Acid”, *Int. J. Recent Trends Eng.*, **1**, pp. 36-40 (2009).
411
- 412 [21] Justnes, H. “Thaumasite followed by sulphate attack on mortar with limestone filler”, *Cem.*
413 *Concr. Compos.*, **25**(8), pp. 955-959 (2003).
414
- 415 [22] Santhanam, M., Cohen, M.D. and Olek, J. “Effects of gypsum formation on the performance
416 of cement mortars during external sulphate attack”, *Cem. Concr. Res.*, **33**(3), pp. 325-332 (2003).
417
- 418 [23] Thokchom, S., Ghosh, P. and Ghosh, S. “Performance of fly ash based geopolymer mortars
419 in sulphate solution”, *J. Eng. Sci. Technol. Rev.*, **3**(1), pp. 36-40 (2010).
420
- 421 [24] Siva Ranjani, G.I. and Ramamurthy, K. “Relative assessment of density and stability of
422 foam produced with four synthetic surfactants”, *Mater. Struct.*, **43**(10), pp. 1317-1325 (2010).
423
- 424 [25] Singh, B., Ishwarya, G., Gupta, M. and Bhattacharyya, S.K. “Geopolymer concrete: a
425 review of some recent developments”, *Const. Build. Mater.*, **85**(15), pp. 78-90 (2015).
426
- 427 [26] McGrath, P.F. and Hooton, R.D. “Re-evaluation of the AASHTO T259 90day salt ponding
428 test”, *Cem. Concr. Res.*, **29**(8), pp. 1239-1248 (1999).

429

430 [27] Bernal, S.A., de Gutiérrez, R.M. and Provis, J.L. “Engineering and durability properties of
431 concretes based on alkali-activated granulated blast furnace slag/metakaolin blends”, *Constr.*
432 *Build. Mater.*, **33**, pp. 99-108 (2012).

433

434 [28] Ken, P.W., Ramli, M. and Ban, C.C. “An overview on the influence of various factors on
435 the properties of geopolymer concrete derived from industrial by-products”, *Constr. Build.*
436 *Mater.*, **77**, pp. 370-395 (2015).

437

438 [29] Bakharev, T., Sanjayan, J.G. and Cheng, Y.B. “Hydration of slag activated by alkalis”, *J.*
439 *Aust. Ceram. Soc.*, **34**, pp. 195-200 (1998).

440

441 [30] Yang, T., Yao, X. and Zhang, Z. “Quantification of chloride diffusion in fly ash–slag-based
442 geopolymers by X-ray fluorescence (XRF)”, *Constr. Build. Mater.*, **69**, pp. 109-115 (2014).

443 **Bibliography**

444

445 **Parthiban Kathirvel**, working as Assistant Professor in the School of Civil Engineering,
446 SASTRA University, Thanjavur, India has completed his B.Tech. in Civil Engineering from
447 SASTRA University in the year 2006, M.E. in Computer Methods and Applications in Structural
448 Engineering from Anna University in the year 2008 and M.B.A. in Technology Management
449 from Anna University in the year 2010. He is pursuing his Ph.D. in the area of Geopolymer
450 Concrete.

451

452 **Saravana Raja Mohan Kaliyaperumal**, working as Associate Dean in the School of Civil
453 Engineering, SASTRA University, Thanjavur, India has completed his B.E. in Civil Engineering
454 from Annamalai University in the year 1986, M.E. in Structural Engineering from Annamalai
455 University in the year 1989 and Ph.D. from Bharathidasan University in the year 2006. He is
456 working in the area of Structural Mechanics of Reinforced Concrete members.

457 **Figures and Tables**

458

459 **List of Tables**

460 Table 1. Chemical composition of GGBFS

461 Table 2. Mix proportioning of the AASC mixes

462 Table 3. Chloride Diffusion Coefficient (CDC) results of the AASC mixes

463

464 **List of Figures**

465 Fig 1. Workability results of the AASC mixes

466 Fig 2. 7 days compressive strength results of the AASC mixes

467 Fig 3. 28 days compressive strength results of the AASC mixes

468 Fig 4. Water absorption capacity results of the AASC mixes

469 Fig 5. Volume of permeable voids results of the AASC mixes

470 Fig 6. Variation in mass loss of the AASC mixes under H₂SO₄ attack

471 Fig 7. Variation in strength loss of the AASC mixes under H₂SO₄ attack

472 Fig 8. Variation in mass loss of the AASC mixes under Na₂SO₄ attack

473 Fig 9. Variation in strength loss of the AASC mixes under Na₂SO₄ attack

474 Fig 10. Variation in mass loss of the AASC mixes under MgSO₄ attack

475 Fig 11. Variation in strength loss of the AASC mixes under MgSO₄ attack

476 Fig 12a. Specimens subjected to Na₂SO₄ exposure

477 Fig 12b. Specimens subjected to MgSO₄ exposure

478 Fig 13. Chloride content profile for the AASC mixes with L/B = 0.45

479 Fig 14. Chloride content profile for the AASC mixes with L/B = 0.50

480 Fig 15. Chloride content profile for the AASC mixes with L/B = 0.55

481

482 Table 1. Chemical composition of GGBFS

Oxide	CaO	SiO ₂	Al ₂ O ₃	MgO	SO ₃	Fe ₂ O ₃	Na ₂ O	K ₂ O
GGBFS (%)	36.77	30.97	17.41	9.01	1.82	1.03	0.69	0.46

483

484

485 Table 2. Mix proportioning of the AASC mixes

Mix label	Slag content	Fine aggregate	Coarse aggregate	NaOH solution	Na ₂ SiO ₃ solution
Mix proportions (kg/m ³)					
AAS350	350	450	1422	58.33	116.67
AAS400	400	432	1368	66.67	133.33
AAS450	450	415	1313	75	150

486

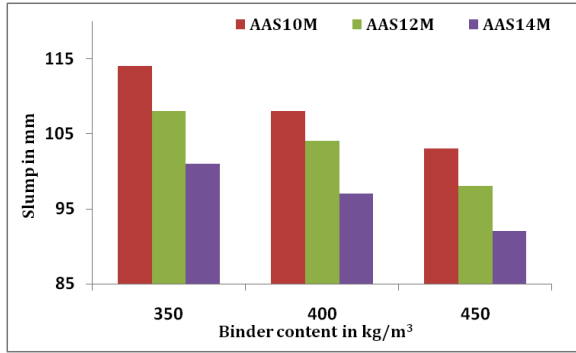
487

488 Table 3. Chloride Diffusion Coefficient (CDC) results of the AASC mixes

Slag content (kg/m ³)	Chloride Diffusion Coefficient in m ² /s (x 10 ⁻¹²)		
	AAS10M	AAS12M	AAS14M
350	2.64	1.84	1.61
400	1.81	1.57	0.88
450	1.56	0.91	0.80

489

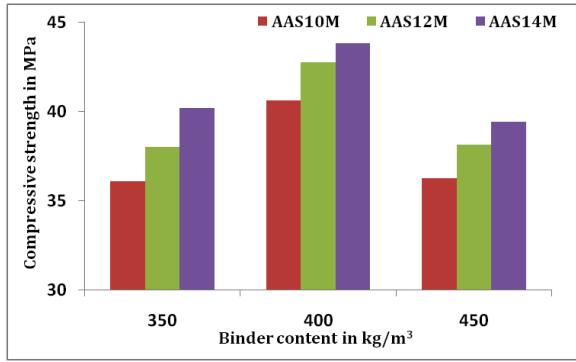
490



491

492 Fig 1. Workability results of the AASC mixes

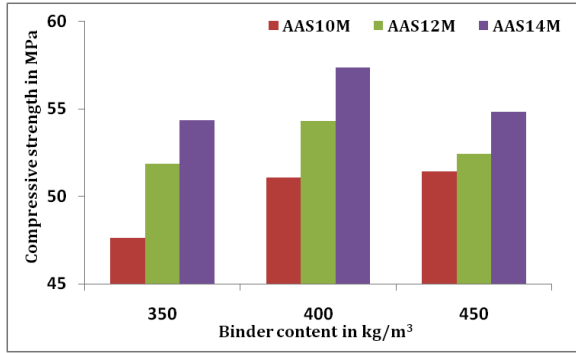
493



494

495 Fig 2. 7 days compressive strength results of the AASC mixes

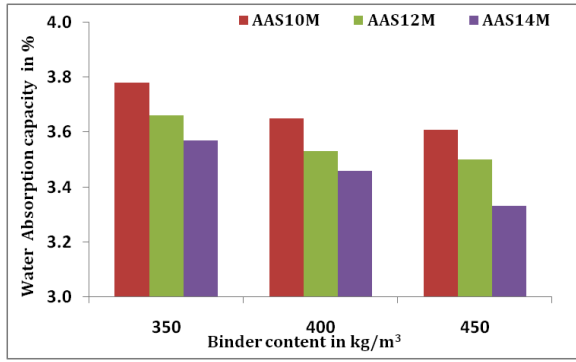
496



497

498 Fig 3. 28 days compressive strength results of the AASC mixes

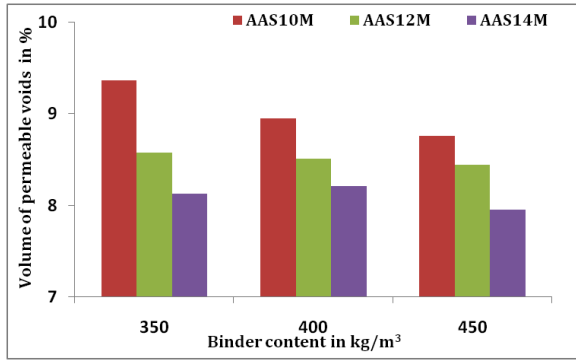
499



500

501 Fig 4. Water absorption capacity results of the AASC mixes

502

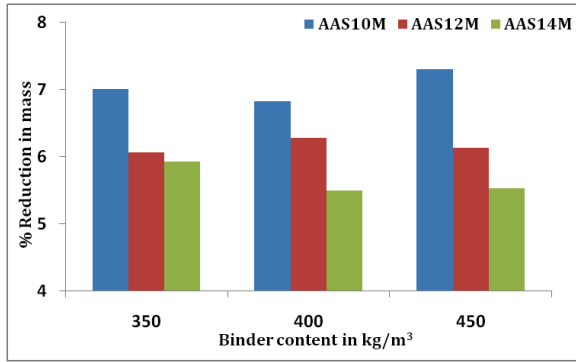


503

504

Fig 5. Volume of permeable voids results of the AASC mixes

505

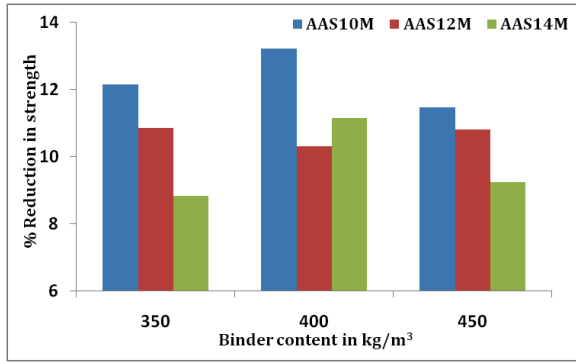


506

507

Fig 6. Variation in mass loss of the AASC mixes under H₂SO₄ attack

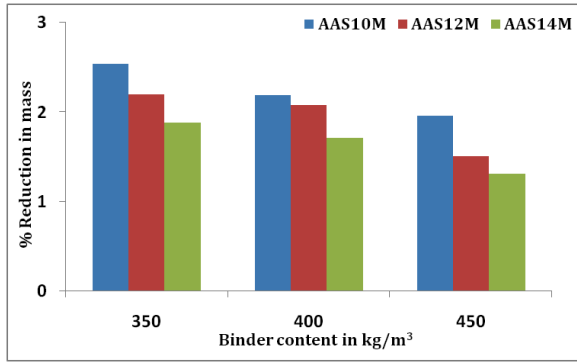
508



509

510 Fig. 7. Variation in strength loss of the AASC mixes under H₂SO₄ attack

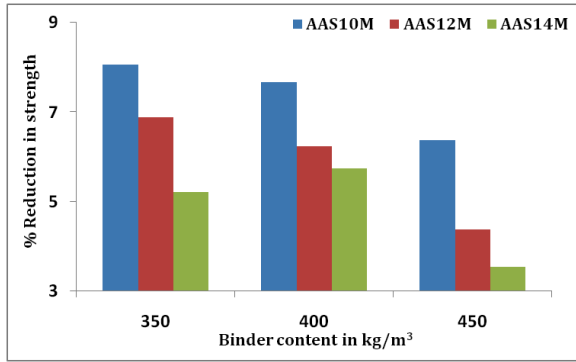
511



512

513 Fig 8. Variation in mass loss of the AASC mixes under Na₂SO₄ attack

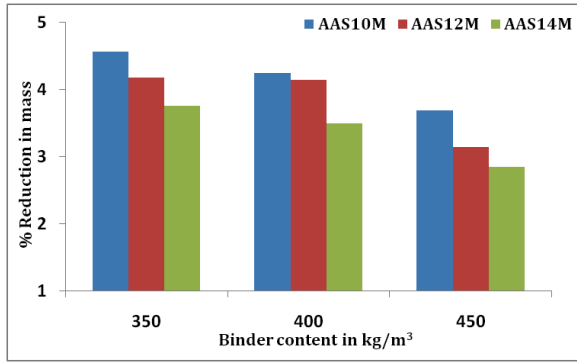
514



515

516 Fig 9. Variation in strength loss of the AASC mixes under Na₂SO₄ attack

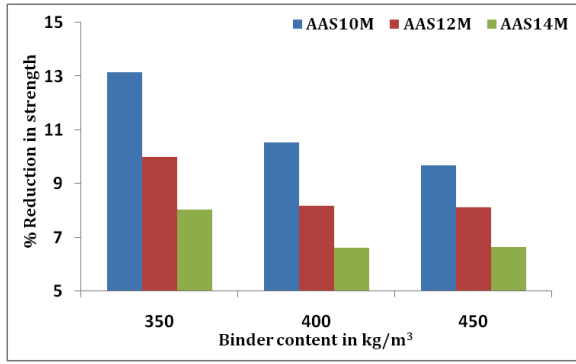
517



518

519 Fig 10. Variation in mass loss of the AASC mixes under MgSO₄ attack

520



521

522 Fig 11. Variation in strength loss of the AASC mixes under MgSO₄ attack

523



524

525 Fig 12a. Specimens subjected to Na_2SO_4 exposure

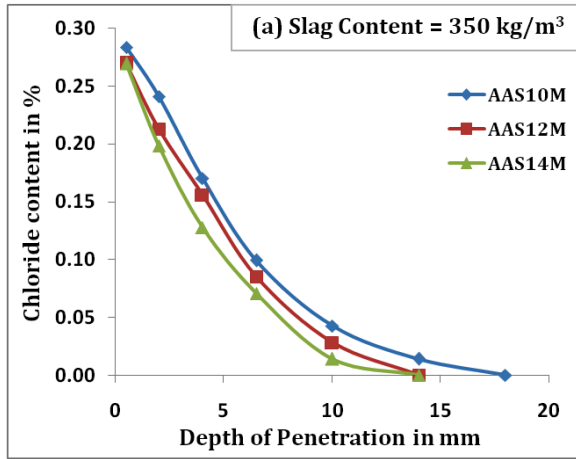
526



527

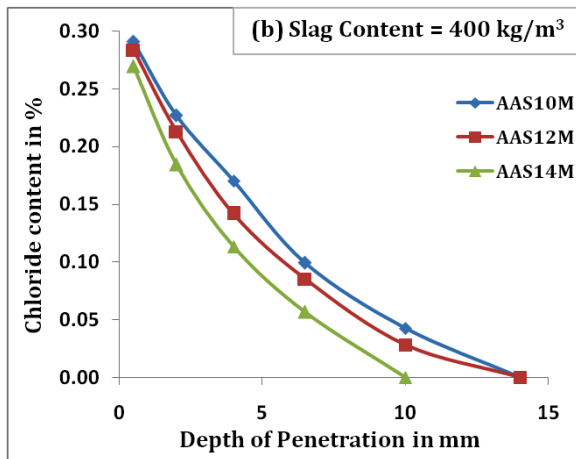
528 Fig 12b. Specimens subjected to MgSO_4 exposure

529



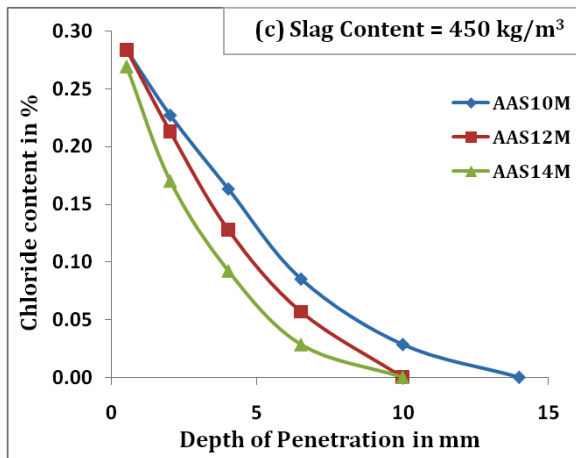
530

531



532

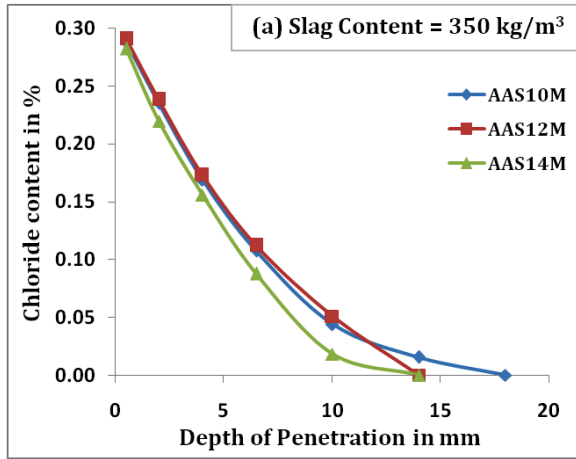
533



534

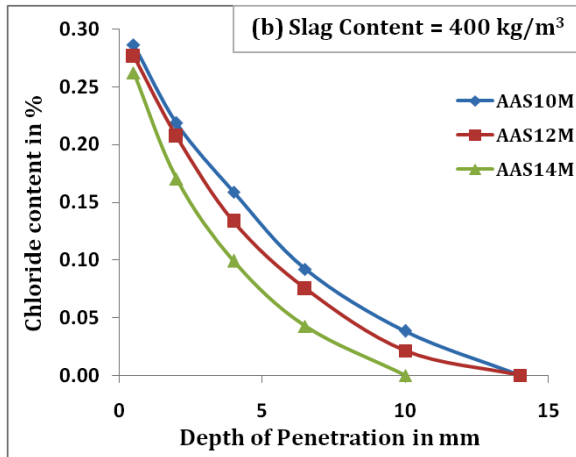
535 Fig 13. Chloride content profile for the AASC mixes with L/B = 0.45

536



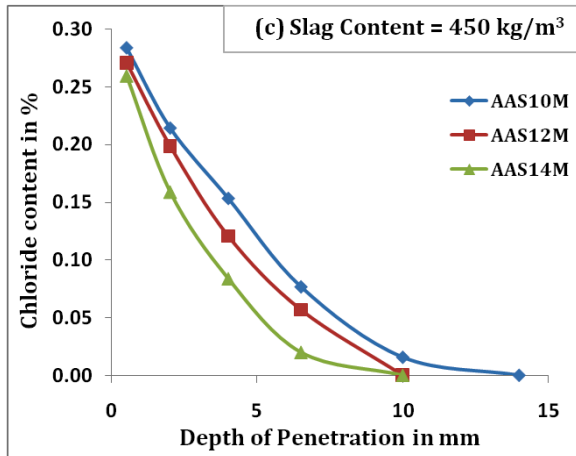
537

538



539

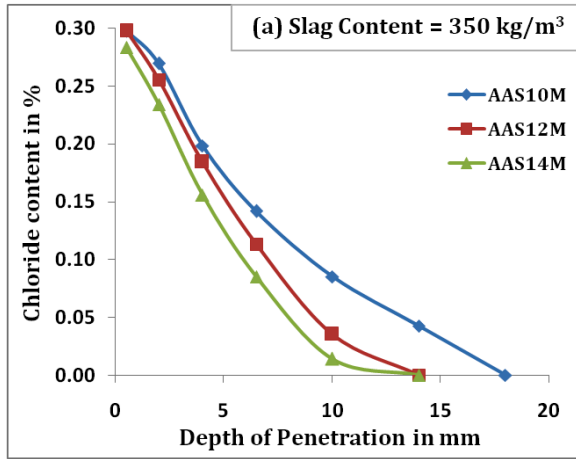
540



541

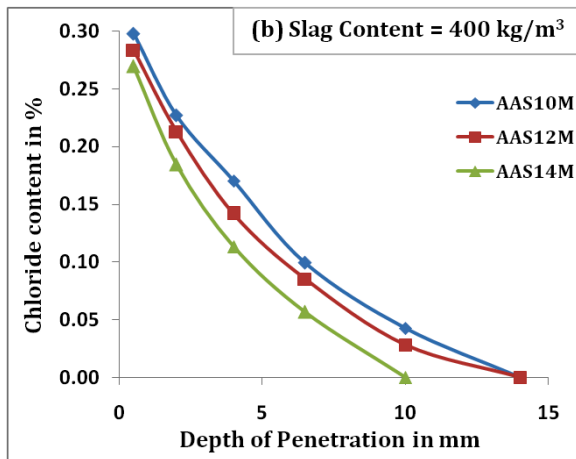
542 Fig 14. Chloride content profile for the AASC mixes with L/B = 0.50

543



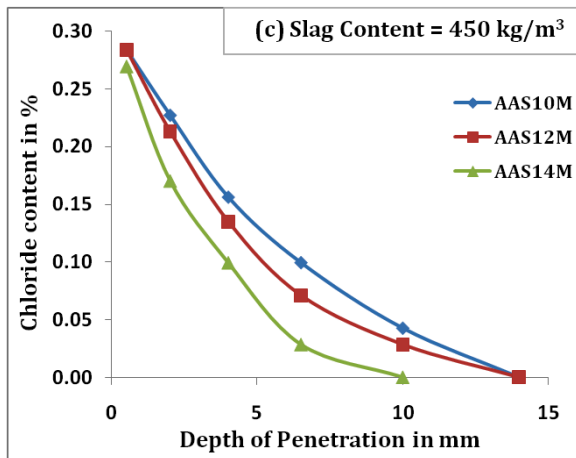
544

545



546

547



548

549 Fig 15. Chloride content profile for the AASC mixes with L/B = 0.55

550